Quaternary Research 83 (2015) 345–354

Contents lists available at ScienceDirect

Quaternary Research

journal homepage: www.elsevier.com/locate/yqres

Stable isotopes in yellow-bellied marmot (*Marmota flaviventris*) fossils reveal environmental stability in the late Quaternary of the Colorado Rocky Mountains

Linda M. Reynard [a,*], David J. Meltzer [b], Steven D. Emslie [c], Noreen Tuross [a]

[a] Department of Human Evolutionary Biology, Harvard University, Cambridge, MA, USA
[b] Department of Anthropology, Southern Methodist University, Dallas, TX 75275, USA
[c] Department of Biology and Marine Biology, University of North Carolina, 601 S. College Road, Wilmington, NC 28403, USA

ARTICLE INFO

Article history:
Received 22 July 2014
Available online 11 February 2015

Keywords:
Bone collagen
Isotope ratios
Oxygen
Hydrogen
Nitrogen
Carbon
Radiocarbon
Last glacial maximum

ABSTRACT

High elevation plant and animal communities are considered extremely sensitive to environmental change. We investigated an exceptional fossil record of yellow-bellied marmot (*Marmota flaviventris*) specimens that was recovered from Cement Creek Cave (elev. 2860 m) and ranged in age from radiocarbon background circa 49.8 cal ka BP to ~1 cal ka BP. We coupled isotopic and radiocarbon measurements ($\delta^{18}O$, δD, $\delta^{15}N$, $\delta^{13}C$, and ^{14}C) of bone collagen from individually-AMS dated specimens of marmots to assess ecological responses by this species to environmental change over time in a high elevation basin in the Rocky Mountains of southwestern Colorado, USA. We find little change in all four isotope ratios over time, demonstrating considerable environmental stability during periods when the marmots were present. The stable ecology and the apparent persistence of the small mammal community in the cave fauna throughout the late Quaternary are in marked contrast to the changes that occurred in the large mammal community, including local extirpation and extinction, at the end of the Pleistocene.

Introduction

The late Quaternary climatic and environmental history of the southern Rocky Mountains is broadly known through multiple proxy indicators from this and adjacent regions. These proxies include speleothems (Asmerom et al., 2010; Wagner et al., 2010), lake cores (Anderson, 2011), pollen and plant macrofossils (Spaulding et al., 1983; Thompson et al., 1993; Fall, 1997a, 1997b; Briles et al., 2012; Cole et al., 2013), fauna (Emslie, 1986, 2002; McLean and Emslie, 2012; McLean et al., 2014), and glacial retreat sequences (Armour et al., 2002; Benson et al., 2005; Brugger, 2007; Guido et al., 2007; Leonard, 2007; Brugger, 2010). Although these data paint a generally consistent picture of changes over time, there is variation in the details.

Of particular interest is the climate and environment of the Upper Gunnison Basin (UGB) of southwestern Colorado, where there is evidence of significant changes in temperature, precipitation and vegetation over the late Quaternary (e.g., Fall, 1997a, 1997b; Brugger, 2007, 2010; Briles et al., 2012), yet apparently long-term stability in the small mammal community (Emslie and Meltzer, 2010; McLean and Emslie, 2012; McLean et al., 2014). Stable isotopic analyses of carbon and oxygen of bioapatite of yellow-bellied marmots (*Marmota flaviventris*) and bushy-tailed woodrats (*Neotoma cinerea*) from Cement Creek Cave in the UGB show no changes in diet across the Pleistocene–Holocene boundary; however, there was a shift in $\delta^{13}C$, which was attributed to changes in atmospheric CO_2 concentration that further influenced the carbon isotope ratio in herbaceous forage plants (McLean and Emslie, 2012).

To obtain further insight into the apparent stability of a high-elevation rodent habitat across major climate events (last glacial maximum, Younger Dryas Chronozone, and the Pleistocene–Holocene transition) during the late Quaternary, we investigated the unique fossil record of marmots from Cement Creek Cave, which spans much of the past ~50 ka. We derived a series of individually-AMS dated specimens to provide better chronological control, and investigated additional stable isotopes (δD, $\delta^{15}N$, $\delta^{18}O$, and $\delta^{13}C$) within bone collagen, in order to resolve differential metabolic and diagenetic effects between tissues (Jim et al., 2004).

The study area

The Upper Gunnison Basin encompasses an 11,000 km^2 area of southwestern Colorado within the southern Rocky Mountains and on the eastern edge of the Colorado Plateau and on the western slope of the Continental Divide (Fig. 1). It has an elevation range of 2200–4300 m and no outlet lower than 2650 m, except through the narrow gorge of the Black Canyon of the Gunnison to the west. This canyon,

* Corresponding author at: Department of Human Evolutionary Biology, 11 Divinity Avenue, Cambridge, MA, 02138, USA.
E-mail address: lreynard@fas.harvard.edu (L.M. Reynard).

http://dx.doi.org/10.1016/j.yqres.2014.12.006
0033-5894/

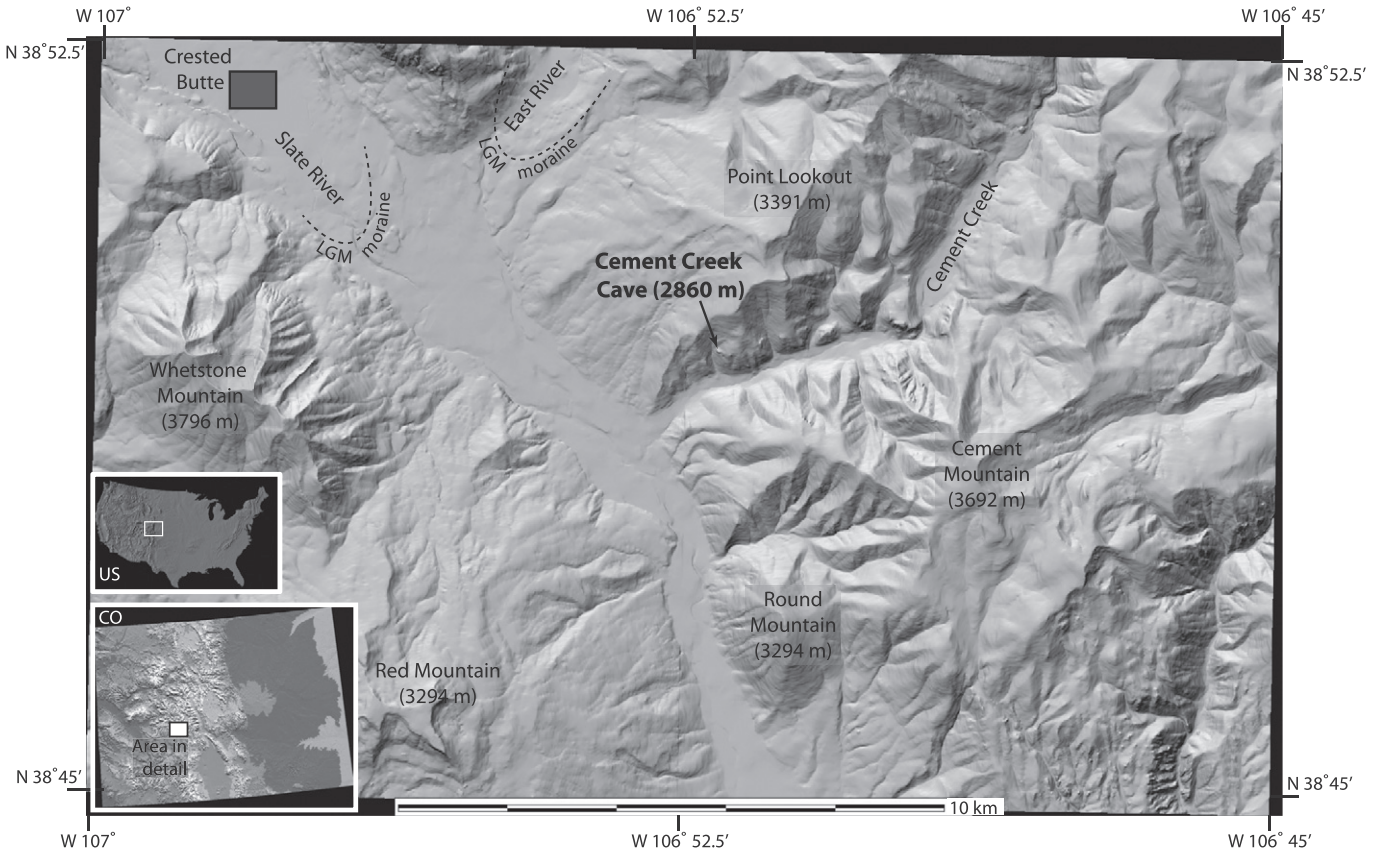

Figure 1. Digital elevation model of the Crested Butte and Cement Creek USGS 7.5' quadrangles, showing the location of Cement Creek Cave in the Upper Gunnison Basin, Colorado, USA (insets). LGM moraine positions are approximate, and based on Brugger (2010, and personal communication 2014).

which includes a 20 km section that is over 700 m deep and only 400 m across at its narrowest point, acts as a filter for the movement of species in and out of the Basin. No other large montane basin in Colorado is enclosed by similar geographic barriers, and it is this feature that probably has caused the development of the unusual climate, communities and biogeographic patterns now present in the Basin (Barrell, 1969; Emslie, 1986; Stiger, 2001).

Existing paleoclimate data

The pertinent paleoclimate data for the UGB and nearby regions are from speleothems from New Mexico and Arizona (Wagner et al., 2010; Asmerom et al., 2010; Polyak et al., 2012) and pollen from lake cores in the southern Rocky Mountains (Fall, 1997a; Anderson, 2011; Briles et al., 2012). The Fort Stanton Cave (New Mexico) speleothem has a high-resolution record of $\delta^{18}O$ and $\delta^{13}C$ from 56 to 11 ka, with a range in $\delta^{18}O$ (calcite) of 5–6‰ (Asmerom et al., 2010; Polyak et al., 2012). At times during the late glacial period, large and rapid changes in temperature and precipitation water source are posited; the latter from more abundant winter Pacific-sourced precipitation (low $\delta^{18}O$) to less abundant summer North American Monsoon precipitation (high $\delta^{18}O$). These data indicate changes in both moisture source and amount as well as temperature in the region from 56 ka onwards (Supplementary Fig. 1). The Cave of the Bells speleothem from Arizona ranges from 54 to 30 ka and 23 to 12 ka and contains isotopic changes between drier winters and warmer temperatures in the interstadials and wetter winters and lower temperatures in the stadials (Wagner et al., 2010). Overall, the regional expression of the last glacial maximum (LGM) was wetter than present (Wagner et al., 2010). Combined $\delta^{13}C$ and $\delta^{234}U$ suggests a strong drought at the end of the Pleistocene in the area (Terminal Pleistocene Drought, Polyak et al., 2012), starting at 14.5 ka. In addition, a less pronounced dry period from 17.5 to 16 cal ka BP, that is correlated with a lowstand in New Mexico's Lake Estancia (Lake Estancia Big Dry, Allen and Anderson, 2000; Broecker et al., 2009; Polyak et al., 2012).

Late Quaternary montane glaciers in the UGB reached their maximum extent from 20.8 to 16.1 ka (Brugger, 2007), consistent with the last glacial maximum in North America of 20 to 19 ka (Clark et al., 2009). The inferred equilibrium-line altitude for the LGM-age Taylor Basin Glacier Complex is 3370 ± 60 m elevation (Brugger, 2007, 2010), significantly higher than the elevation of Cement Creek Cave. Glacial ice was present in the upper reaches of the Cement Creek drainage, but its terminus was well up-valley and at a higher elevation (Brugger, K.A., personal communication, 2010). Glacial lobes came down the Slate and East River valleys and extended past the present town of Crested Butte, Colorado, terminating at an elevation of ~2700 m (Brugger, 2010: Figs. 4 and 5; Brugger personal communication 2014). Although reaching a lower elevation than Cement Creek Cave, these were still >6 km from the entrance to the Cement Creek valley. There is no glacial geomorphic evidence in the Cement Creek valley in the proximity of the cave to suggest it was ever glaciated, a point of relevance in interpreting the radiocarbon chronology (as noted below). The LGM temperatures in the region are estimated to have been 5–7°C lower than at present (Stute et al., 1992; Bartlein et al., 1998; Brugger, 2010).

Pollen from a core obtained from Lily Pond, at 3208 m elevation in the Taylor Basin ~20 km north of Cement Creek Cave, has yielded a local vegetation record starting soon after local deglaciation at 16.8 cal ka BP (Briles et al., 2012). This basal zone shows mixed tundra and subalpine parkland. From 14.7 cal ka BP a subalpine forest developed, with generally warmer temperatures (Asmerom et al., 2010). This forest persisted through the Younger Dryas Chronozone 12.9–11.7 cal ka BP, and other nearby pollen records show shifts from tundra to subalpine forest, suggesting little or no return to cooler conditions (Fall, 1997a, 1997b; Briles et al., 2012). The early Holocene featured increased pine forest, while

the middle Holocene pollen indicates a return to subalpine forests, with greater summer temperatures. Calcite $\delta^{18}O$ values from 3255 m elevation Bison Lake (Upper Colorado River Basin, ~110 km from Cement Creek) indicate that the mid to late Holocene features lower summer temperatures, and increased snowfall relative to rain (Anderson, 2011). Overall these climate data show variability that may have affected small mammals such as marmots in alpine environments.

Bones as an environmental sample

While speleothem isotopic composition offers potentially high resolution paleoclimatic data, their use is restricted to karstic environments. They are influenced by the site-specific soil and environmental conditions (Fairchild and Treble, 2009) and non-equilibrium processes (Coplen, 2007; Day and Henderson, 2011), and may not be relevant to the region of interest. Given that animal bones are present in many contexts, they present another sample set for stable isotope measurement and inferred paleoclimate evidence. The difficulty with deriving precise environmental information from bones, on the other hand, is that one is constrained by the age of the samples available and many samples are needed for adequate time resolution.

Isotopic analysis of mammal tooth enamel and bone (carbonate and phosphate) has been used to reconstruct past temperatures and ecosystems (Navarro et al., 2004; McLean and Emslie, 2012). However, few studies have used bone collagen, and fewer still oxygen and hydrogen isotope ratios from collagen (e.g., Cormie et al., 1994; Leyden et al., 2006; Kirsanow et al., 2008; Reynard and Hedges, 2008). Bone collagen is a useful tissue because one can obtain both radiocarbon dates and up to five different isotope ratios from aliquots of the same sample, and in some cases bone remains are far more abundant than tooth enamel. In addition, in small animals the limited amount of tooth enamel can preclude carbonate or phosphate $\delta^{18}O$ analysis, and the interpretation of laser-ablation $\delta^{18}O$ data is far from straightforward.

Excavations in Cement Creek Cave yielded diverse taxa of small mammals, most abundantly represented by *M. flaviventris* which occurred in nearly all excavation levels in the cave deposits. We also chose to study this species as marmots adequately represent high-elevation small mammal communities in the southern Rocky Mountains. Marmots hibernate in winter; in subalpine areas this is presently from September to May, though emergence is earlier at lower elevations (February to mid-March). In some lower elevation populations, summer estivation occurs, though this is not noted in boreal groups. Marmots inhabit vegetated slopes or meadows, and consume a diet that includes grasses, forbs, flowers, and seeds (Frase and Hoffman, 1980).

Previous analysis of carbonate $\delta^{18}O$ and $\delta^{13}C$ from marmots and bushy-tailed woodrats (*N. cinerea*) from Cement Creek Cave showed little change in $\delta^{18}O$ over time, and a decrease in $\delta^{13}C$ into the Holocene, which was hypothesized to be a result of increasing atmospheric CO_2 concentration (McLean and Emslie, 2012). However, bone collagen is composed of differing proportions of drinking water and food macronutrients than carbonate and thus may more fully capture environmental change (Tieszen and Fagre, 1993; Kirsanow and Tuross, 2011). In addition, while previous work by McLean and Emslie (2012) relied on an age-depth model of excavation levels to obtain a chronology for their analysis, stratigraphic mixing limits the resolution of that chronology. Hence, we individually AMS-radiocarbon dated each bone subjected to stable isotope ratio measurement, thereby providing high chronological resolution for the resulting data, an additional strong advantage of using bone collagen as an environmental sample.

Isotope ratios in bone collagen

Over glacial–interglacial changes, measureable variation in faunal bone collagen $\delta^{15}N$ and $\delta^{13}C$ of a few per mil has been noted (Iacumin et al., 2000; Drucker et al., 2003; Richards and Hedges, 2003; Stevens and Hedges, 2004; Iacumin et al., 2010; Szpak et al., 2010). The former is attributed to changes in soil nitrogen more broadly, and the latter primarily to changes in atmospheric CO_2 concentration ($\delta^{13}C$ of atmospheric CO_2 changed only slightly over the last 25 ka, by ~0.3‰, Schmitt et al., 2012). It is therefore probable that mammal bone collagen will reflect large environmental changes, such as the Pleistocene–Holocene transition.

Several factors affect collagen isotope ratios. Beginning with plants, $\delta^{15}N$ and $\delta^{13}C$ can vary substantially (Fraser et al., 2011; Warinner et al., 2013), due to factors including aridity, soil type, ecosystem, and plant photosynthetic type and N-fixing (Heaton, 1987, 1999). These isotopic differences can then lead to differences in consumer bone collagen isotope ratios. $\delta^{13}C$ varies the most between C_3, C_4, or CAM plants, and thus $\delta^{13}C$ of the plant diet affects consumer collagen $\delta^{13}C$, either directly or indirectly via meat consumption (Vogel and van der Merwe, 1977; DeNiro and Epstein, 1978). At a given location and narrow time period, $\delta^{15}N$ and δD may increase broadly with trophic level (Minagawa and Wada, 1984; Birchall et al., 2005; Hedges and Reynard, 2007; Reynard and Hedges, 2008). In vertebrates $\delta^{18}O$ varies by species, due to differences in metabolic rate and water use (Bryant and Froehlich, 1995). $\delta^{18}O$ and δD also vary geographically as a function of precipitation isotope ratio, due to distance from the oceanic water source, amount of precipitation rained out, and temperature (Dansgaard, 1964; Criss, 1999). As a result the use of bone collagen for environmental studies must control carefully for these factors to eliminate dietary, geographic, and species-dependent effects.

Methods

The site

Cement Creek Cave is a solution cavity within a discontinuous outcrop of Leadville limestone (Paleozoic, Middle Mississippian age), at 2860 m elevation, south of the town of Crested Butte, CO (Fig. 1). The cave has a south-facing, relatively small (<1 m diameter) circular opening that at present is ~3 m above the outside ground surface, which itself is ~200 m above the Cement Creek valley floor. Once through the entrance, the cave opens into a small antechamber, from which there are several shafts (some closed at this time) extending into the mountainside. What appears at present as the main passageway extends

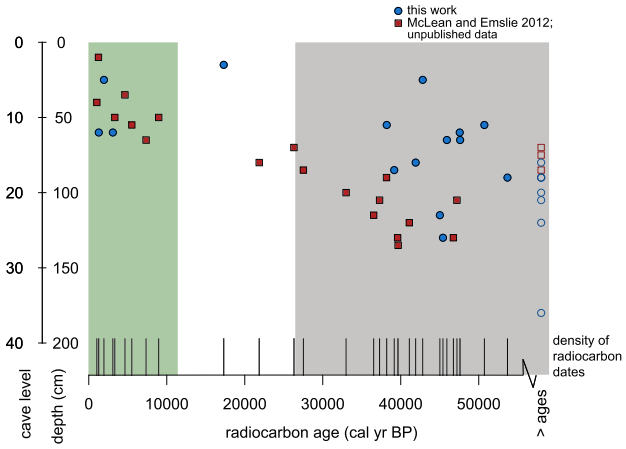

Figure 2. Radiocarbon dates (cal yr BP) and density of sampling of marmots from Cement Creek Cave as a function of cave level and total depth. Background (greater than) radiocarbon ages are given by open symbols. The shading delineates Holocene (green), LGM and late Wisconsin (unshaded), and pre-LGM (gray) time periods. The global onset of the LGM at 26.5 ka is used as a boundary (Clark et al., 2009). The local Upper Gunnison Basin maximum glaciation is at 20.8–16.1 ka (Brugger, 2007), while the global end of the LGM is estimated at 20–19 ka (Clark et al., 2009).
Data are from this work (circles), McLean and Emslie (2012) and unpublished results (squares).

Table 1
Isotope, elemental, and radiocarbon data for marmots from Cement Creek Cave.

Lab code	Level	Trench	Element	$\delta^{18}O_{SMOW\text{-}SLAP}$		$\delta D_{SMOW\text{-}SLAP}$		n	atomic	$\delta^{15}N_{AIR}$		$\delta^{13}C_{VPDB}$		atomic	n	^{14}C lab	^{14}C age	±	mean, μ	95% conf. interval	
				(‰)		(‰)		(O,H)	O/H	(‰)		(‰).....		C/N	(C,N)	code	(^{14}C yr BP)		(cal yr BP)[a]	(cal yr BP)[a]	
	8	TP1	Li1									−22.0				Beta 128214	1120	40	1033	1174	938
	2	TP2 NE	Lm3									−20.9	0.1			UCIAMS 53285	1300	15	1240	1285	1183
CC2-12-39	12	TP2	Right mandible	10.7	0.4	−70	1.5	3	0.298	3.3	0.2	−21.2	0.2	3.29	2	UCIAMS 137893	1345	20	1282	1305	1192
CC2-5-38	5	TP2	Right mandible	8.6	0.7	−96	4.9	5	0.298	3.7	0.2	−20.8	0.0	3.31	2	UCIAMS 137891	1995	20	1944	1992	1896
CC2-12-2	12	TP2	Right maxilla	9.6	0.4	−87	0.3	2	0.301	4.0	0.1	−20.9	0.2	3.32	2	UCIAMS 126399	2935	25	3088	3168	2998
	10	TP2 NE	LM1 or 2									−20.8	0.1			UCIAMS 53287	3120	15	3338	3383	3260
	7	TP2 NE	RM1 or 2									−20.7	0.1			UCIAMS 53286	4105	15	4641	4801	4528
	11	TP2 NE	Molar									−20.1	0.1			UCIAMS 56844	4780	20	5520	5588	5473
	13	TP2 NE	Left mandible, i1									−21.2	0.1			UCIAMS 56845	6400	20	7342	7417	7271
	10	TP1	LI1									−20.8				Beta 125777	8070	50	8965	9130	8768
CC2-3-8	3	TP2	Left radius	10.5	0.2	−67	1.3	2	0.301	3.1	0.2	−20.0	0.1	3.30	2	UCIAMS 137890	14,210	60	17,303	17,512	17,092
	16	TP2 NE	Rm3									−19.5	0.1			UCIAMS 53288	18,040	70	21,855	22,104	21,604
	14	TP2 NE	Left i1									−20.8				UGAMS 10621	22,110	55	26,311	26,550	26,091
	17	TP2 NE	Left premaxilla									−19.6	0.1			UCIAMS 85361	23,260	120	27,514	27,726	27,303
	20	TP1	Left tibia									−23.6				Beta 129369	28,820	180	32,989	33,556	32,410
	23	TP2 NE	LM2									−20.3	0.1			UCIAMS 53291	32,440	430	36,532	37,872	35,449
	21	TP2 NE	LI									−19.8	0.1			UCIAMS 85362	33,060	410	37,288	38,395	36,260
	18	TP2 NE	Lm3									−20.4	0.1			UCIAMS 53290	33,840	510	38,175	39,505	36,745
CC2-11-10	11	TP2	Juv. left femur	8.6	0.4	−74	0.7	3	0.304	2.6	0.0	−20.4	0.1	3.30	2	UCIAMS 137892	33,860	620	38,205	39,755	36,565
CC2-17-40	17	TP2	Left mandible	10.3	0.1	−70	2.2	2	0.304	4.7	0.0	−19.9	0.1	3.32	2	UCIAMS 139606	34,580	810	39,163	41,098	37,097
	26	TP1	Left innominate									−21.7				Beta 120098	34,980	600	39,604	40,975	38,415
	27	TP2 NE	Rm1, jaw									−20.6	0.1			UCIAMS 53293	35,040	590	39,662	40,988	38,478
	24	TP2 NE	Lm2 or 3									−20.6	0.1			UCIAMS 53292	36,560	720	41,099	42,330	39,795
CC2-16-14	16	TP2	Left scapula	9.2		−73		1	0.324	3.6	0.0	−20.2	0.0	3.38	2	UCIAMS 137894	37,510	980	41,915	43,568	40,187
CC2-5-9	5	TP2	Left humerus	9.9	0.4	−71	6.2	4	0.313	2.7	0.2	−20.3	0.1	3.38	2	UCIAMS 139603	38,400	1300	42,818	45,254	40,599
CC2-23-19	23	TP2	Right ilium	8.2	0.5	−84	4.7	3	0.331	2.1	0.0	−21.5	0.2	3.43	2	UCIAMS 137898	41,000	1500	45,018	48,245	42,458
CC2N-26-30	26	TP2 NE Ext.	Left humerus	10.9	0.4	−69	6.3	4	0.308	2.8	0.5	−20.4	0.2	3.35	2	UCIAMS 137900	41,400	1600	45,414	48,813	42,682
CC2-13-3	13	TP2	Right humerus	8.4	0.5	−90	6.0	3	0.310	5.4	0.1	−20.1	0.1	3.31	2	UCIAMS 126400	42,000	1600	45,917	49,212	43,140
	17	TP2 NE	Rm3									−20.6	0.1			UCIAMS 53289	>43,300		46,424		

CC2-18-17	18	TP2	Left humerus	8.9	0.3	−74	3.7	2	0.337	2.3	0.1	−20.7	0.2	3.47	2	UCIAMS 139607	>43,400		46,521		
	26	TP1	Left I1									−20.0				Beta 135140	43,330	760	46,748	48,494	45,229
	15	TP2 NE	Rm3, mandible									−20.5	0.1			UCIAMS 56847	>43,900		47,056		
CC2N-18-25	18	TP2 NE Ext.	Juv. left radius	11.9	0.7	−73	11.3	4	0.322	2.8	0.0	−20.1	0.1	3.36	2	UCIAMS 139608	>47,200				
	21	TP2 NE	LM1									−20.5	0.1			UCIAMS 53294	43,700	1900	47,208		44,741
CC2-20-18	20	TP2	Right femur	10.0	0.9	−71	4.8	4	0.307	3.5	0.3	−21.3	0.1	3.33	2	UCIAMS 137896	>44,200		47,402		
CC2-12-11	12	TP2	Left radius	8.5	1.2	−71	4.1	4	0.307	3.7	0.1	−20.0	0.2	3.27	2	UCIAMS 139604	45,100	3000	47,565		44,799
CC2-13-12	13	TP2	Right calcaneum	10.4	0.4	−73	3.5	3	0.308	3.1	0.1	−20.6	0.0	3.32	2	UCIAMS 139605	45,300	3100	47,614		44,857
CC2N-16-4	16	TP2 NE Ext	Right innominate						0.321	2.3	0.1	−20.3	0.1	3.47	2	UCIAMS 126396	>44,400		47,637		
	14	TP2 NE	Molar									−20.9	0.1			UCIAMS 56846	>44,800		48,128		
CC2N-21-27	21	TP2 NE Ext.	Right humerus	9.7	0.2	−84	4.7	2	0.315	3.9	0.0	−20.5	0.2	3.39	2	UCIAMS 137897	>48,500				
CC2N-24-29	24	TP2 NE Ext.	Right premaxilla	10.2	0.0	−82	5.5	2	0.308	2.8	0.1	−19.9	0.1	3.34	2	UCIAMS 137899	>49,200				
CC2-18-41	18	TP2	Left mandible	9.9	0.5	−65	7.5	3	0.309	3.1	0.1	−20.2	0.2	3.36	2	UCIAMS 137895	>46,400		49,767		
CC2N-36-48	36	TP2 NE Ext.	Left mandible	8.8	0.2	−68	5.0	2	0.350	3.5	0.1	−20.1	0.4	3.37	2	UCIAMS 137901	>46,400		49,767		
CC2-11-1	11	TP2	Left tibia	9.1	0.8	−71	9.2	4	0.307	5.9	0.5	−20.2	0.2	3.28	2	UCIAMS 126398	47,700	3200	50,723	62,581	42,788
CC2N-18-5	18	TP2 NE Ext	Left innominate	9.3	0.4	−79	2.0	3	0.304	2.9	0.1	−20.1	0.0	3.28	2	UCIAMS 126397	49,100	3800	53,683	68,773	43,887
CC2-15-13	15	TP2	Juv. Left femur	9.6	0.3	−79	7.7	3	0.316	4.1	0.1	−20.8	0.1	3.65	2						
CC2N-20-26	20	TP2 NE Ext.	Right ulna	9.5	0.5	−71	4.9	3	0.305	4.0	0.2	−20.5	0.1	3.33	2						
CC2N-23-28	23	TP2 NE Ext.	Left humerus	7.4	0.3	−77	4.3	3	0.302	5.2	0.2	−20.5	0.2	3.30	2						
CC2N-32-34	32	TP2 NE Ext.	Left radius	9.4	0.4	−72	0.8	2	0.308	2.9	0.2	−20.4	0.2	3.37	2						
CC2N-37-37	37	TP2 NE Ext.	Tibia	8.7	0.4	−63	5.3	2	0.298	3.0	0.1	−20.1	0.1	3.61	2						
CC2-32-23	32	TP2	Right humerus	6.8	0.0	−82	0.5	2	0.336	2.9	0.0	−21.0	0.0	3.64	2						
CC2-26-44	26	TP2	Left mandible	5.9		−64		1	0.407	2.3	0.1	−20.9	0.0	3.56	2						
CC2-17-16	17	TP2	Juv. left femur	8.0		−51			0.435	1.7	0.0	−20.1	0.2	3.54	2						
CC2-25-43	25	TP2	Right mandible	5.1	0.1	−70	0.9	2	0.493	2.1		−20.7		3.49	1						
CC2N-11-45	11	TP2 NE Ext.	Right mandible	4.7	0.3	−79	3.5	2	0.517	3.2	0.1	−20.7	0.2	3.83	2						
CC2-16-15	16	TP2	Left mandible	5.9		−73		1	0.527	3.7	0.1	−20.4	0.4	3.35	2						
CC2-2-7	2	TP2	Right tibia	5.6		−81			0.539	3.0	0.1	−20.3	0.1	3.63	2						
CC2N-34-47	34	TP2 NE Ext.	Right mandible	3.9		−67		1	0.653	3.1	0.1	−21.1	0.0	3.51	2						
CC2-31-22	31	TP2	Left femur	1.6		−58		1	0.808	2.6		−20.9		3.54	1						

[a] Calibrated with Oxcal v. 4.2 (Bronk Ramsey, 2009) using IntCal13 calibration curve (Reimer et al., 2013).

from the antechamber downward ~12 m on a ~30° slope toward the north, where it then levels out into a small, relatively low-ceilinged inner chamber of ~3 m in diameter. Although additional shafts continue from this spot, this inner chamber serves as a topographic 'collection point' for any sediment or fossil material that might have rolled or washed down the passageway from the entrance and antechamber, as well as a center of rodent activity, especially that of the bushy-tailed woodrat (*N. cinerea*) and its middens.

Sediments on the floor of this chamber were initially tested in 1998 when a 50 × 50 cm test pit (TP1) was excavated to a depth of 1.3 m in 10 cm arbitrary levels (Emslie, 2002). In 2007, a 1 × 1.5 m excavation was completed in 5-cm levels to a depth 2 m (40 levels) below surface (TP2 and TP2 NE). The excavated sediments were screened through three stacked screens with mesh sizes, from top to bottom, of 0.64, 0.32, and 0.025 cm^2 (the last fraction was water-screened). This process resulted in the recovery of thousands of bones from each level, primarily of small mammals with some bird remains as well (Emslie and Meltzer, 2010). It is this more recently excavated sample from Cement Creek Cave that yielded the marmot remains used in the analysis reported here, as well as a wealth of other small mammals representing high-elevation alpine and subalpine environments.

Based on present day indications, as well as the recovered vertebrate remains, it would appear that Cement Creek Cave was occupied — and the faunal assemblages accumulated — primarily by rodents and small carnivores (e.g., mustelids; Emslie and Meltzer, 2010) as well as owls and other raptors depositing pellets at the cave entrance (Emslie and Meltzer, 2010). Accordingly, most of the species represented in this assemblage likely occurred within a relatively short distance from the cave. Although individual skeletal elements of Pleistocene large mammals such as bison, horse and shrub-ox occur occasionally in these deposits, these were likely brought in by rodents. There are no signs that medium- to large-size mammals (including humans, who were present in the UGB in late Pleistocene times [Stiger, 2006; Meltzer, unpublished]) ever occupied the cave, probably due to its high (3 m above the outside surface level), small entrance.

Stable isotope and radiocarbon measurements

Marmot bones were demineralized over several weeks in 0.5 M EDTA (Tuross et al., 1988; Tuross, 2012), rinsed in deionized water, and subsequently separated into aliquots for stable isotope analysis and radiocarbon dating. The former was freeze-dried with no further preparation. The radiocarbon aliquot was gelatinized overnight in slightly acidic deionized water, filtered through a quartz filter, and freeze-dried (Tuross, 2012). Known background age bones served as process blanks. Samples were dated at the Keck Carbon Cycle AMS at UC Irvine. Radiocarbon dates were calibrated with OxCal version 4.2 (Bronk Ramsey, 2009) using the IntCal13 calibration curve (Reimer et al., 2013).

Isotope ratios were measured on a Thermo-Finnegan Delta Plus XP, coupled to a Costech 1040 elemental analyzer (C and N) and a Thermo thermal-conversion elemental analyzer (O and H), the latter as described in Tuross et al. (2008). SMOW and SLAP were used directly as reference materials (in silver divots, USGS) and all $\delta^{18}O$ and δD data are normalized to the SMOW-SLAP scale. All samples were measured in an 8-day period, to minimize the effect of changing atmospheric vapor δD on collagen δD, and an internal laboratory standard collagen was run with each batch to ensure this effect was negligible. Water–collagen exchange experiments were also performed on a subset of samples to determine the influence of environmental water on measured collagen δD. The extent of water exchange is small enough that any variability in environmental water isotopic ratio has a minimal effect on measured collagen δD (Supplementary data).

We excluded samples with atomic C/N greater than 3.6 (n = 5) from further analysis, since ratios greater than 3.6 indicate likely diagenetic alteration (DeNiro, 1985). The use of O/H ratios to determine the extent of diagenetic alteration has not undergone systematic study; however, our work on this project and others suggest that atomic O/H ratios of >0.35 as determined on our TC/EA-mass spectrometer combination indicate diagenetic alteration (Supplementary Fig. 2). Most samples cluster tightly, but a few depart toward higher O/H ratios. We measured O/H of 0.31–0.33 in modern calf skin Type I collagen, which is similar to most of the samples reported in Table 1. In the Cement Creek collagens, samples with higher O/H are correlated with and result in significantly lower $\delta^{18}O$ values (Supplementary Fig. 3). More samples are excluded based on O/H ratios (n = 8), which indicate that it is a more sensitive indicator of diagenetic alteration than C/N ratios, though three samples were excluded based on C/N ratios and not O/H. Two samples only were excluded on the basis of both C/N and O/H ratios.

Results

A total of 45 radiocarbon ages have been completed on fossil marmots (Table 1) and span a range from 1033 cal yr BP (95% range 1174–938) to ^{14}C background of >49,200 ^{14}C yr BP (Fig. 2). As can be seen, these are distributed in a somewhat bimodal fashion, with the majority ($n = 32$) predating 26,500 cal yr BP (the global onset of the LGM as given by relative sea level, Clark et al., 2009), less than half that number ($n = 10$) postdating 10,000 ^{14}C yr BP, with the few remaining falling within the temporal bounds of the LGM or shortly thereafter ($n = 3$; Fig. 2). Dating of other species recovered from Cement Creek likewise showed a reduction in specimens that fall within the LGM period, but that result is based on a smaller number of specimens ($n = 14$) and would require additional dating to confirm (unpublished data). As noted above, this is not a function of the cave being sealed by glacial ice during the LGM. However, it is conceivable that access to its interior was limited during much (though not all) of the LGM: its entrance, as also noted, is relatively small and could have easily been sealed and/or the surrounding area covered by snow and ice during wetter glacial times. Regardless, we caution that there are few data points during the last glacial maximum when it is likely that the Upper Gunnison Basin experienced the greatest climatic and ecological perturbation.

$\delta^{18}O$ values range from 8.2 to 11.9‰, with a mean of 9.6 ± 0.9‰ ($n = 23$, ±1 SD, Fig. 3a). There is no significant difference between <10 and >10 cal ka BP data (Welch *t* test, p = 0.97, means 9.6 ± 1.1‰ and 9.6 ± 0.9‰, respectively). Summary statistics for $\delta^{18}O$, δD, $\delta^{15}N$, and $\delta^{13}C$ are given in Table 2. δD and $\delta^{15}N$ do not vary with time (Table 2, Figs. 3b,c), but $\delta^{13}C$ shows a small but significant difference between pre- and post-10 cal ka BP (p = 0.009), with means of −21.0 ± 0.2‰ and −20.3 ± 0.4‰, respectively (Fig. 3d, with the $\delta^{13}C$ values from this study only). As a consequence of the taphonomy of the site, several samples from the upper layers in fact dated to the pre-LGM period, resulting in few Holocene-aged samples with all four isotope ratios available (Table 1), but reinforcing the need to utilize only individually-dated samples.

The $\delta^{13}C$ values were also generated for all 45 marmot samples incidentally to radiocarbon dating (Fig. 3d). The mean $\delta^{13}C$ is −20.9‰ for ages <10 cal ka BP vs. −20.5‰ for ages >10 cal ka BP, still a significant difference (Welch *t* test, p = 0.02), but essentially identical to the smaller $\delta^{13}C$ data set, indicating that the latter is robust.

Discussion

Remarkably, we found no significant oxygen, hydrogen, and nitrogen isotopic change in our samples over time. The $\delta^{18}O$ in bone collagen of the animals measured at Cement Creek Cave does not vary significantly through time, though a 3.7‰ range is seen. Controlled animal experiments on rats and woodrats have shown that changes in the isotopic ratio of drinking water is differentially reflected in various tissues (Podlesak et al., 2008; Kirsanow and Tuross, 2011). In rats, 57% of a given $\delta^{18}O$ difference in drinking water is measured in bone

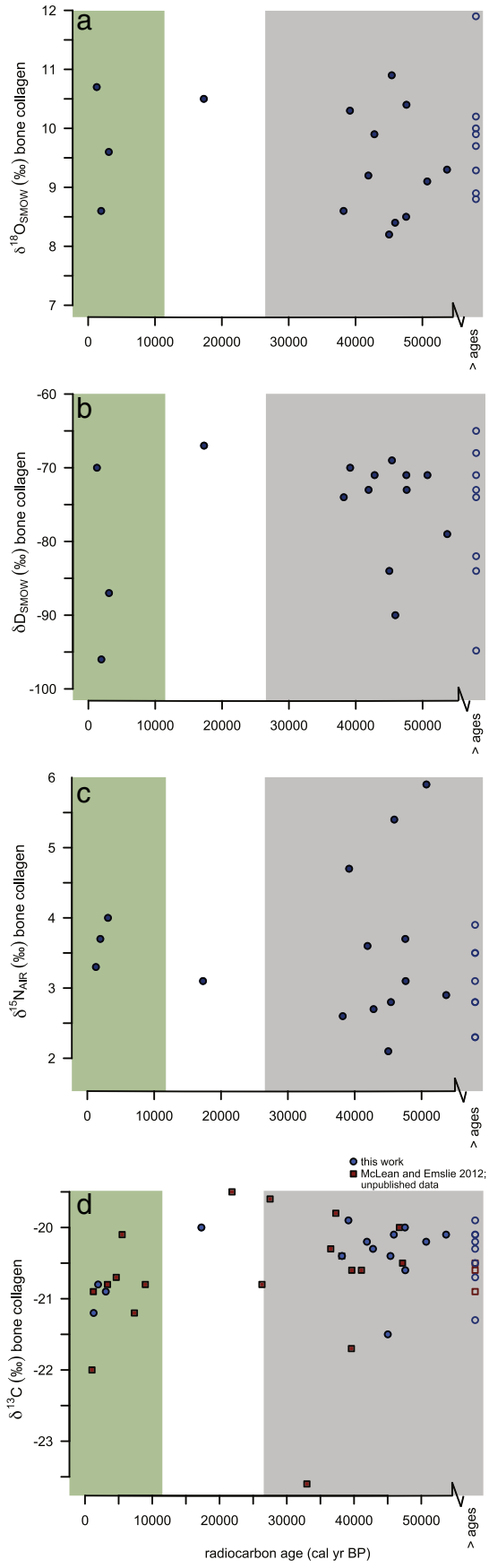

Table 2
Summary statistics for marmot $\delta^{18}O_{SMOW}$, δD_{SMOW}, $\delta^{15}N_{AIR}$, and $\delta^{13}C_{VPDB}$.

	All (n = 23)		<10 cal ka BP (n = 3)		>10 cal ka BP (n = 20)		*t* Test
	Mean	SD	Mean	1 SD	Mean	1 SD	p
$\delta^{18}O$	9.6	0.9	9.6	1.1	9.6	0.9	0.97
δD	−76	9.0	−84	13	−75	8	0.35
$\delta^{15}N$	3.4	0.9	3.7	0.4	3.3	1.0	0.31
$\delta^{13}C$	−20.4	0.5	−21.0	0.2	−20.3	0.4	0.009
$\delta^{13}C$ (all)[a]	−20.5	0.5	−20.9	0.5	−20.5	0.5	0.02

[a] n = 44 total from all AMS radiocarbon analyses, n = 10 for ages < 10 cal ka BP, n = 34 ages > 10 cal ka BP; one $\delta^{13}C = -23.6‰$ outlier excluded; the difference in $\delta^{13}C$ is also significant with the outlier point included (p = 0.005).

collagen (i.e., for each 1‰ change in drinking water, bone collagen changes by 0.57‰); for δD, only 15% of a water isotopic difference is reflected in bone collagen (Kirsanow and Tuross, 2011). In these rats, collagen $\delta^{18}O$ captures slightly greater differences in water source values than enamel carbonates, which are often used for paleoecological studies (57% vs. 43%, respectively, Kirsanow and Tuross, 2011). These experimental animals had controlled diets that were purposefully isotopically different from drinking water. In most real-world scenarios, the food O and H isotopic composition may be related to that of local water, so that the effects of changes in environmental water on tissues may be greater than these estimates. In free-ranging ovicaprids, serially-sampled dentin collagen captured 71% of the annual change in $\delta^{18}O$ and 49% of δD, significantly larger than the controlled feeding experiments (Kirsanow et al., 2008). These animals differ from small rodents in body size and possibly also in the relative amounts of food vs. water consumed. Further work on multiple isotope ratios from bone collagen of small mammals in free-ranging settings (as opposed to large-bodied animals or controlled experimental settings) will be useful to determine more precisely how strongly each isotope ratio reflects environmental inputs and change.

Assuming that the animal experiments are a valid model, the 3.7‰ range in bone collagen $\delta^{18}O$ seen here is equivalent to drinking water changes of 6.5‰ (3.7‰/0.57). This range corresponds to ~4.5°C temperature differences (Dansgaard, 1964), neglecting all other influences on $\delta^{18}O$. Marmots hibernate in the fall and winter and are active in the spring and summer (Frase and Hoffman, 1980), and thus are incorporating the water available at that time of year into biomass, including presumably a high proportion of snow-melt derived water, especially in the spring and early summer. Climate models for the period from 21 to 14 ka suggest that summer temperatures changed far more than winter temperatures (Bartlein et al., 1998), so a bias to winter precipitation could mean a dampened temperature response. The relative contribution of snowpack melt vs. rainfall precipitation at high altitude Bison Lake in the Colorado Rocky Mountains varied through the Holocene, as reflected in changes in lake sedimentary calcite $\delta^{18}O$ (Anderson, 2011). If this were the case throughout the Pleistocene as well, this would add to variability in marmot $\delta^{18}O$. Similarly, the polar jet stream has moved northward/southward through the stadials/interstadials (Wagner et al., 2010; Asmerom et al., 2010), leading to changes in either total precipitation (Wagner et al., 2010) or the relative amount of Pacific winter precipitation vs. North American Monsoon summer precipitation, with different $\delta^{18}O$ source values (Asmerom et al., 2010), in some parts of

Figure 3. Stable isotope ratios as a function of radiocarbon date (cal yr BP) for marmot bone collagen. Background (greater than) radiocarbon ages are given by open circles. The shading delineates Holocene (green), LGM and late Wisconsin (unshaded), and pre-LGM (gray) time periods. Three isotope ratios a) $\delta^{18}O_{SMOW}$ (‰), b) δD_{SMOW} (‰), c) $\delta^{15}N_{AIR}$ (‰) show no significant difference between the Holocene and other time periods. $\delta^{13}C_{VPDB}$ (‰) (panel d) shows a small (0.4‰) but significant (p = 0.02) difference in $\delta^{13}C$ between the Holocene and later time periods.
Data are from this work (circles); McLean and Emslie (2012) and unpublished results (squares).

the US southwest. These three potential factors (temperature, snowpack contributions to local waters, and precipitation source) may influence marmot $\delta^{18}O$ values and result in the variability seen here.

Carbonate $\delta^{18}O$ from Cement Creek Cave marmot teeth interquartile ranges are from ~23.0 to 30.5‰ (converted relative to SMOW, McLean and Emslie, 2012), which is more than twice the 3.7‰ range found in collagen. However, there is no pattern of change over time in $\delta^{18}O$ carbonate. This ~7.5‰ range is relatively high, particularly if only 43% of drinking water change is captured in carbonate (animal experiments, Kirsanow and Tuross, 2011). Additional parameters other than changing drinking water isotopic composition, such as animal growth and development and/or some diagenetic overprinting are likely causing the range in variation in $\delta^{18}O$ measured in marmot carbonate.

The mean carbonate $\delta^{18}O$ (26.8‰ relative to SMOW, estimated by the mid-point of the maximum and minimum interquartile ranges, McLean and Emslie, 2012) is 17.2‰ greater than the mean collagen $\delta^{18}O$, which is slightly higher than the 14.1–14.9‰ difference found in controlled feeding studies of rats (Kirsanow and Tuross, 2011) and 15.1–15.2‰ in pigs (Warinner and Tuross, 2009). Nonetheless this compares favorably given that this is an uncontrolled wild population, and suggests that collagen $\delta^{18}O$ is regularly related to carbonate $\delta^{18}O$.

We find here a range in δD of 31‰; this compares to a similar δD range of up to 27‰ in bone collagen for Holocene bison within various sites near to each other in Saskatchewan (Leyden et al., 2006). Those data show very weak changes through the Holocene using site means; it appears that for making climate-related inferences with bone collagen δD some form of binning or averaging is required. Over very broad geographical scales collagen δD is related to precipitation δD (Cormie et al., 1994; Reynard and Hedges, 2008); however, in the Cement Creek Cave marmots collagen δD and $\delta^{18}O$ are very weakly correlated ($r^2 = 0.17$, $p = 0.05$), so are not representing precipitation isotopic composition in the same manner. This is perhaps unsurprising given the different contribution of both water and food to collagen δD and $\delta^{18}O$.

Bone collagen $\delta^{15}N$ in some cases varies temporally within a species, particularly pre- and post-LGM. European fauna such as reindeer, horse, and bison show a few per mil change in bone collagen $\delta^{15}N$ over the last 50 ka (Richards and Hedges, 2003; Drucker et al., 2003; Stevens and Hedges, 2004). Siberian mammoths at 12–13 ^{14}C ka BP have ~3.5‰ lower $\delta^{15}N$ than before the LGM (Iacumin et al., 2010), while some Eurasian mammoths and reindeer have ~2–3‰ lower $\delta^{15}N$ between 25–20 ka and 15 ka (Iacumin et al., 2000). There is considerable geographical heterogeneity in the existence or magnitude of this change in $\delta^{15}N$, however (Iacumin et al., 2000; Szpak et al., 2010). In contrast to these examples, we find little change in $\delta^{15}N$ here; we infer more consistency in the subalpine environment inhabited by these marmots, with less change in soil chemistry that is then reflected in plant $\delta^{15}N$ and thus faunal bone collagen over this timescale. An additional difference is that the previous work sampled large-bodied mobile grazers, with longer life-spans and greater geographical ranges than small-bodied rodents, which might then result in more averaged bone collagen isotope ratios, smoothing out some of the seasonal and inter-annual variability.

The slight difference in bone collagen $\delta^{13}C$ pre- and post-10 cal ka BP (0.5–0.7‰) is less than the ~2‰ Pleistocene to Holocene enamel carbonate difference (McLean and Emslie, 2012; McLean et al., 2014). Carbonate in bioapatite is formed from blood bicarbonate, which reflects whole diet and metabolism while collagen carbon may be biased toward protein-derived carbon, but also includes carbon from other dietary macronutrients (Tieszen and Fagre, 1993; Jim et al., 2004). Thus, it is perhaps not surprising that the magnitude of change over time is different in these two different tissues in the Cement Creek Cave marmots. The marmot collagen $\delta^{13}C$ is consistent with C_3 plant consumption throughout the entire time period represented here, and the small shift in the carbon isotopic composition in bone collagen between the Pleistocene and Holocene individuals could derive from a number of changes in environmental parameters such as CO_2 levels, changes in plant stomatal conductance, change in the $\delta^{13}C$ in air or small shifts in the distribution of the plant community (e.g., Schubert and Jahren, 2012). Some of the other studies of faunal bone collagen $\delta^{13}C$ through the last ~50 ka have also not found any change over time (Iacumin et al., 2000; Drucker et al., 2003).

Conclusions

This is one of the first investigations to couple collagen radiocarbon dates with a quartet of organic light stable isotopes (H, O, C and N), each of which is subject to different environmental impacts and constraints, from the same species to evaluate environmental change through time. These data show little change in marmot bone collagen and thus inferred environment, when they are present at Cement Creek Cave, from radiocarbon background age of ~49 to 1 cal ka BP. The distribution of radiocarbon dates shows a gap in marmot and other small mammal presence in the range 30–10 cal ka BP, overlapping the local last glacial maximum. As each isotope ratio is reflective of dietary and environmental parameters in slightly different ways, the congruence of all four reinforces the picture of ecological stability relative to marmots in this subalpine environment, particularly during the periods before and after the LGM. The concurrence of bioapatite and collagen carbon and oxygen isotopic trends in this population further supports the interpretation of environmental equivalence during the times when the marmots utilized the cave.

These results are surprising given that high-elevation communities are thought to be more sensitive to environmental change, and thus more susceptible to extinctions during major climatic events. Certainly the large mammal fauna of the UGB suffered considerable extinctions and turnover with loss of megafauna, similar to other regions of North America (Emslie, 1986; Gill et al., 2009). However, the small mammal community as a whole at Cement Creek Cave from the end of the late Quaternary into the early Holocene reflects only one extinction (the short-faced skunk, *Brachyprotoma* sp.) and three extirpations (*Sorex preblei*, *Lemmiscus curtatus*, and until recent re-invasion, *Urocitellus elegans*; Emslie and Meltzer, 2010). From the perspective of the marmot populations, the consistent isotopic values reflect stability in this high altitude environment for much of the late glacial period.

Acknowledgments

Excavations in Cement Creek Cave were conducted under Special Use Permit FS-2700-4 from the U.S. Forest Service. Funding was provided by NSF Grant EAR 0819678 (to Emslie and Meltzer) and the Quest Archaeological Research Program at Southern Methodist University (Meltzer). We thank A. Boehm, M. Eren, L. Reeder, and L. Willis for assistance in the field and laboratory. M. Stiger provided laboratory space at Western State Colorado University (Gunnison) for screen washing of the sediments. K. Brugger aided our efforts to understand the glacial geology of the Upper Gunnison Basin. Radiocarbon dates were completed by J. Southon, Univ. of California Irving Keck Carbon Cycle AMS Facility. B. McLean provided useful comments on an earlier version of this manuscript.

Appendix A. Supplementary data

Supplementary data to this article can be found online at http://dx.doi.org/10.1016/j.yqres.2014.12.006.

References

Allen, B., Anderson, R., 2000. A continuous, high-resolution record of late Pleistocene climate variability from the Estancia Basin, New Mexico. Geological Society of America Bulletin 112, 1444–1458.

Anderson, L., 2011. Holocene record of precipitation seasonality from lake calcite ^{18}O in the Central Rocky Mountains, United States. Geology 39, 211–214.

Armour, J., Fawcett, P., Geissman, J., 2002. 15 k.y. paleoclimatic and glacial record from northern New Mexico. Geology 30, 723–726.

Asmerom, Y., Polyak, V.J., Burns, S.J., 2010. Variable winter moisture in the southwestern United States linked to rapid glacial climate shifts. Nature Geoscience 3, 114–117.

Barrell, J., 1969. Flora of the Gunnison Basin. Natural Land Institute, Rockford, Illinois.

Bartlein, P., Anderson, K., Anderson, P., Edwards, M., Mock, C., Thompson, R., Webb, R., Whitlock, C., 1998. Paleoclimate simulations for North America over the past 21,000 years: features of the simulated climate and comparisons with paleoenvironmental data. Quaternary Science Reviews 17, 549–585.

Benson, L., Madole, R., Landis, G., Gosse, J., 2005. New data for Late Pleistocene Pinedale alpine glaciation from southwestern Colorado. Quaternary Science Reviews 24, 49–65.

Birchall, J., O'Connell, T.C., Heaton, T.H.E., Hedges, R.E.M., 2005. Hydrogen isotope ratios in animal body protein reflect trophic level. Journal of Animal Ecology 74, 877–881.

Briles, C.E., Whitlock, C., Meltzer, D.J., 2012. Last glacial–interglacial environments in the southern Rocky Mountains, USA and implications for Younger Dryas-age human occupation. Quaternary Research 77, 96–103.

Broecker, W.S., McGee, D., Adams, K.D., Cheng, H., Edwards, R.L., Oviatt, C.G., Quade, J., 2009. A Great Basin-wide dry episode during the first half of the Mystery Interval? Quaternary Science Reviews 28, 2557–2563.

Bronk Ramsey, C., 2009. Bayesian analysis of radiocarbon dates. Radiocarbon 51, 337–360.

Brugger, K.A., 2007. Cosmogenic ^{10}Be and ^{36}Cl ages from Late Pleistocene terminal moraine complexes in the Taylor River drainage basin, central Colorado, USA. Quaternary Science Reviews 26, 494–499.

Brugger, K.A., 2010. Climate in the Southern Sawatch Range and Elk Mountains, Colorado, USA, during the Last Glacial Maximum: inferences using a simple degree–day model. Arctic, Antarctic, and Alpine Research 42, 164–178.

Bryant, J.D., Froehlich, P.N., 1995. A model of oxygen isotope fractionation in body water of large animals. Geochimica et Cosmochimica Acta 59, 4523–4537.

Clark, P.U., Dyke, A.S., Shakun, J.D., Carlson, A.E., Clark, J., Wohlfarth, B., Mitrovica, J.X., Hostetler, S.W., McCabe, A.M., 2009. The Last Glacial Maximum. Science 325, 710–714.

Cole, K., Fisher, J., Ironside, K., Mead, J., Koehler, P., 2013. The biogeographic histories of *Pinus edulis* and *Pinus monophylla* over the last 50,000 years. Quaternary International 310, 96–110.

Coplen, T.B., 2007. Calibration of the calcite–water oxygen-isotope geothermometer at Devils Hole, Nevada, a natural laboratory. Geochimica et Cosmochimica Acta 71, 3948–3957.

Cormie, A.B., Schwarcz, A.P., Gray, J., 1994. Relation between hydrogen isotopic ratios of bone collagen and rain. Geochimica et Cosmochimica Acta 58, 377–391.

Criss, R.E., 1999. Principles of Stable Isotope Distribution. Oxford University Press, Oxford.

Dansgaard, W., 1964. Stable isotopes in precipitation. Tellus 4, 436–468.

Day, C.C., Henderson, G.M., 2011. Oxygen isotopes in calcite grown under cave-analogue conditions. Geochimica et Cosmochimica Acta 75, 3956–3972.

DeNiro, M.J., 1985. Postmortem preservation and alteration of in vivo bone collagen isotope ratios in relation to palaeodietary reconstruction. Nature 317, 806–809.

DeNiro, M.J., Epstein, S., 1978. Influence of diet on distribution of carbon isotopes in animals. Geochimica et Cosmochimica Acta 42, 495–506.

Drucker, D.G., Bocherens, H., Billiou, D., 2003. Evidence for shifting environmental conditions in Southwestern France from 33000 to 15000 years ago derived from carbon-13 and nitrogen-15 natural abundances in collagen of large herbivores. Earth and Planetary Science Letters 216, 163–173.

Emslie, S.D., 1986. Late Pleistocene vertebrates from Gunnison County, Colorado. Journal of Paleontology 60, 170–176.

Emslie, S.D., 2002. Fossil shrews (Insectivora: Soricidae) from the late Pleistocene of Colorado. Southwestern Naturalist 47, 62–69.

Emslie, S.D., Meltzer, D.J., 2010. A unique high-elevation fossil assemblage spanning the Last Glacial Maximum from Cement Creek Cave, Colorado. Poster presented at the 21st Biennial American Quaternary Association Meeting, Laramie, WY.

Fairchild, I.J., Treble, P.C., 2009. Trace elements in speleothems as recorders of environmental change. Quaternary Science Reviews 28, 449–468.

Fall, P., 1997a. Timberline fluctuations and late Quaternary paleoclimates in the southern Rocky Mountains, Colorado. Geological Society of America Bulletin 109, 1306–1320.

Fall, P., 1997b. Fire history and composition of the subalpine forest of western Colorado during the Holocene. Journal of Biogeography 24, 309–325.

Frase, B.A., Hoffman, R.S., 1980. Marmota flaviventris. Mammalian Species 135, 1–8.

Fraser, R.A., Bogaard, A., Heaton, T., Charles, M., Jones, G., Christensen, B.T., Halstead, P., Merbach, I., Poulton, P.R., Sparkes, D., Styring, A.K., 2011. Manuring and stable nitrogen isotope ratios in cereals and pulses: towards a new archaeobotanical approach to the inference of land use and dietary practices. Journal of Archaeological Science 38, 2790–2804.

Gill, J.L., Williams, J.W., Jackson, S.T., Lininger, K.B., Robinson, G.S., 2009. Pleistocene megafaunal collapse, novel plant communities, and enhanced fire regimes in North America. Science 326, 1100–1103.

Guido, Z., Ward, D., Anderson, R., 2007. Pacing the post-Last Glacial Maximum demise of the Animas Valley glacier and the San Juan Mountain ice cap, Colorado. Geology 35, 739–742.

Heaton, T.H.E., 1987. The ^{15}N/^{14}N ratio of plants in South Africa and Namibia: relationship to climate and coastal/saline environments. Oecologia 74, 236–246.

Heaton, T.H.E., 1999. Spatial, species, and temporal variations in the ^{13}C/^{12}C Ratios of C_3 plants: implications for palaeodiet studies. Journal of Archaeological Science 26, 637–649.

Hedges, R.E.M., Reynard, L.M., 2007. Nitrogen isotopes and the trophic level of humans in archaeology. Journal of Archaeological Science 34, 1240–1251.

Iacumin, P., Nikolaev, V., Ramigni, M., 2000. C and N stable isotope measurements on Eurasian fossil mammals, 40000 to 10000 years BP: herbivore physiologies and palaeoenvironmental reconstruction. Palaeogeography, Palaeoclimatology, Palaeoecology 163, 33–47.

Iacumin, P., Di Matteo, A., Nikolaev, V., Kuznetsova, T.V., 2010. Climate information from C, N and O stable isotope analyses of mammoth bones from northern Siberia. Quaternary International 212, 206–212.

Jim, S., Ambrose, S., Evershed, R., 2004. Stable carbon isotopic evidence for differences in the dietary origin of bone cholesterol, collagen and apatite: implications for their use in palaeodietary reconstruction. Geochimica et Cosmochimica Acta 68, 61–72.

Kirsanow, K., Tuross, N., 2011. Oxygen and hydrogen isotopes in rodent tissues: impact of diet, water and ontogeny. Palaeogeography, Palaeoclimatology, Palaeoecology 310, 9–16.

Kirsanow, K., Makarewicz, C., Tuross, N., 2008. Stable oxygen (δ^{18}O) and hydrogen (δD) isotopes in ovicaprid dentinal collagen record seasonal variation. Journal of Archaeological Science 35, 3159–3167.

Leonard, E., 2007. Modeled patterns of Late Pleistocene glacier inception and growth in the Southern and Central Rocky Mountains, USA: sensitivity to climate change and paleoclimatic implications. Quaternary Science Reviews 26, 2152–2166.

Leyden, J.J., Wassenaar, L.I., Hobson, K.A., Walker, E.G., 2006. Stable hydrogen isotopes of bison bone collagen as a proxy for Holocene climate on the Northern Great Plains. Palaeogeography, Palaeoclimatology, Palaeoecology 239, 87–99.

McLean, B.S., Emslie, S.D., 2012. Stable isotopes reflect the ecological stability of two high-elevation mammals from the late Quaternary of Colorado. Quaternary Research 77, 408–417.

McLean, B.S., Ward, J.K., Polito, M.J., Emslie, S.D., 2014. Responses of high-elevation herbaceous plant assemblages to low glacial CO_2 concentrations revealed by fossil marmot (Marmota) teeth. Oecologia 175, 1117–1127.

Minagawa, M., Wada, E., 1984. Stepwise enrichment of ^{15}N along food chains: further evidence and the relation between δ^{15}N and animal age. Geochimica et Cosmochimica Acta 48, 1135–1140.

Navarro, N., Lécuyer, C., Montuire, S., Langlois, C., Martineau, F., 2004. Oxygen isotope compositions of phosphate from arvicoline teeth and quaternary climatic changes, Gigny, French Jura. Quaternary Research 62, 172–182.

Podlesak, D.W., Torregrossa, A.M., Ehleringer, J.R., Dearing, M.D., Passey, B.H., Cerling, T.E., 2008. Turnover of oxygen and hydrogen isotopes in the body water, CO_2, hair, and enamel of a small mammal. Geochimica et Cosmochimica Acta 72, 19–35.

Polyak, V.J., Asmerom, Y., Burns, S.J., Lachniet, M.S., 2012. Climatic backdrop to the terminal Pleistocene extinction of North American mammals. Geology 40, 1023–1026.

Reimer, P.J., Bard, E., Bayliss, A., Beck, J.W., Blackwell, P.G., Ramsey, C.B., Buck, C.E., Cheng, H., Edwards, R.L., Friedrich, M., Grootes, P.M., Guilderson, T.P., Haflidason, H., Hajdas, I., Hatte, C., Heaton, T.J., Hoffmann, D.L., Hogg, A.G., Hughen, K.A., Kaiser, K.F., Kromer, B., Manning, S.W., Niu, M., Reimer, R.W., Richards, D.A., Scott, E.M., Southon, J.R., Staff, R.A., Turney, C.S.M., van der Plicht, J., 2013. IntCal13 and Marine13 radiocarbon age calibration curves 0–50,000 years cal BP. Radiocarbon 55, 1869–1887.

Reynard, L.M., Hedges, R.E.M., 2008. Stable hydrogen isotopes of bone collagen in palaeodietary and palaeoenvironmental reconstruction. Journal of Archaeological Science 35, 1934–1942.

Richards, M.P., Hedges, R.E.M., 2003. Variations in bone collagen δ^{13}C and δ^{15}N values of fauna from Northwest Europe over the last 40000 years. Palaeogeography, Palaeoclimatology, Palaeoecology 193, 261–267.

Schmitt, J., Schneider, R., Elsig, J., Leuenberger, D., Lourantou, A., Chappellaz, J., Köhler, P., Joos, F., Stocker, T.F., Leuenberger, M., Fischer, H., 2012. Carbon isotope constraints on the deglacial CO_2 rise from ice cores. Science 336, 711–714.

Schubert, B.A., Jahren, A.H., 2012. The effect of atmospheric CO_2 concentration on carbon isotope fractionation in C_3 land plants. Geochimica et Cosmochimica Acta 96, 29–43.

Spaulding, W.G., Leopold, E.B., Van Devender, T.R., 1983. Late Wisconsin paleoecology of the American Southwest. In: Porter, S. (Ed.), Late-Quaternary Environments of the United States. The Late Pleistocene vol. 1. University of Minnesota Press, Minneapolis, pp. 259–293.

Stevens, R.E., Hedges, R.E.M., 2004. Carbon and nitrogen stable isotope analysis of northwest European horse bone and tooth collagen, 40,000 BP–present: palaeoclimatic interpretations. Quaternary Science Reviews 23, 977–991.

Stiger, M., 2001. Hunter–gatherer Archaeology of the Colorado High Country. University Press of Colorado, Boulder.

Stiger, M., 2006. A Folsom structure in the Colorado mountains. American Antiquity 71, 321–351.

Stute, M., Schlosser, P., Clark, J., Broecker, W., 1992. Paleotemperatures in the Southwestern United States derived from noble-gases in ground-water. Science 256, 1000–1003.

Szpak, P., Groecke, D.R., Debruyne, R., MacPhee, R.D.E., Guthrie, R.D., Froese, D., Zazula, G.D., Patterson, W.P., Poinar, H.N., 2010. Regional differences in bone collagen δ^{13}C and δ^{15}N of Pleistocene mammoths: implications for paleoecology of the mammoth steppe. Palaeogeography, Palaeoclimatology, Palaeoecology 286, 88–96.

Thompson, R.S., Whitlock, C., Bartlein, P.J., Harrison, S.P., Spaulding, W.G., 1993. Climate change in the western United States since 18,000 yr B.P. In: Wright Jr., H.E., Kutzbach, J.E., Webb III, T., Ruddiman, W.F., Street-Perrott, F.A., Bartlein, P.J. (Eds.), Global Climates Since the Last Glacial Maximum. University of Minnesota Press, Minneapolis, pp. 468–513.

Tieszen, L.L., Fagre, T., 1993. Effect of diet quality and composition on the isotopic composition of respiratory CO_2, bone collagen, bioapatite, and soft tissues. In: Lambert, J.B., Grupe, G. (Eds.), Prehistoric Human Bone: Archaeology at the Molecular Level. Springer-Verlag, Berlin, pp. 121–155.

Tuross, N., 2012. Comparative decalcification methods, radiocarbon dates, and stable isotopes of the VIRI bones. Radiocarbon 54, 837–844.

Tuross, N., Fogel, M.L., Hare, P.E., 1988. Variability in the preservation of the isotopic composition of collagen from fossil bone. Geochimica et Cosmochimica Acta 52, 929–935.

Tuross, N., Warinner, C., Kirsanow, K., Kester, C., 2008. Organic oxygen and hydrogen isotopes in a porcine controlled dietary study. Rapid Communications in Mass Spectrometry 22, 1741–1745.
Vogel, J.C., van der Merwe, N.J., 1977. Isotopic evidence for early maize cultivation in New York State. American Antiquity 42, 238–242.
Wagner, J.D.M., Cole, J.E., Beck, J.W., Patchett, P.J., Henderson, G.M., Barnett, H.R., 2010. Moisture variability in the Southwestern United States linked to abrupt Glacial climate change. Nature Geoscience 3, 110–113.
Warinner, C., Tuross, N., 2009. Alkaline cooking and stable isotope tissue-diet spacing in swine: archaeological implications. Journal of Archaeological Science 36, 1690–1697.
Warinner, C., Robles Garcia, N., Tuross, N., 2013. Maize, beans and the floral isotopic diversity of Highland Oaxaca, Mexico. Journal of Archaeological Science 40, 868–873.